С343б
В-24

3/IX -

ОБЪЕДИНЕННЫЙ
ИНСТИТУТ
ЯДЕРНЫХ
ИССЛЕДОВАНИЙ
ДУБНА

3210/2-73

E2 - 7278

V.S.Barashenkov, F.G.Gereghi ,
A.S.Iljinov, V.D.Toneev

INELASTIC INTERACTIONS OF HIGH ENERGY NUCLEONS WITH HEAVY NUCLEI

1973

ЛАБОРАТОРИЯ ЯДЕРНЫХ РЕАНЦИЙ

E2 - 7278

V.S.Barashenkov, F.G.Gereghi [1],
A.S.Iljinov, V.D.Toneev [2]

INELASTIC INTERACTIONS OF HIGH ENERGY NUCLEONS WITH HEAVY NUCLEI

Submitted *to Nuclear Physics*

[1] The Institute of Applied Physics of the Academy of Sciences of the Moldavian Soviet Socialist Republic, Kishinev.

[2] JINR, Laboratory of Theoretical Physics.

Объединенный институт ядерных исследований БИБЛИОТЕКА

Барашенков В.С., Жереги Ф.Г., Ильинов А.С., Тонеев В.Д.

E2 - 7278

Неупругие взаимодействия нуклонов высоких энергий с тяжелыми ядрами

Модель внутриядерных каскадов, учитывающая изменение плотности числа внутриядерных нуклонов в ходе каскада, применяется к расчету взаимодействий протонов с тяжелыми делящимися ядрами в области энергий, больших нескольких десятков Гэв. Результаты расчетов хорошо согласуются с опытом.

Препринт Объединенного института ядерных исследований.
Дубна, 1973

Barashenkov V.S., Gereghi F.G.,
Iljinov A.S., Toneev V.D.

E2 - 7278

Inelastic Interactions of High Energy Nucleons with Heavy Nuclei

The intranuclear cascade model including the effect of changes in the properties of the target nucleus due to development of the shower of cascade particles is applied to calculations of the interactions of protons with fissioning nuclei in the energy region $T \simeq 0.1 - 30$ GeV. The fission cross sections, yields of different isotopes after evaporation stage, and the characteristics of accompanying particles are calculated. The properties of the excited evaporating and fissioning residual nuclei are discussed. The calculated results are compared with experiment.

**Preprint. Joint Institute for Nuclear Research.
Dubna, 1973**

1. INTRODUCTION

A study of the interaction of fast particles with heavy fissioning nuclei is not solely of theoretical interest, but is also of great importance in connection with its application to development of the electronuclear method of producing atomic energy and accumulating rare isotopes [1]. Calculations of these interactions have been done in our work [2] as well as in a number of other papers (see, e.g. refs.[3-8] for further bibliography). However none of these papers can be considered satisfactory in the sense that many of them have made use of a rather approximate model of a nucleus with a sharp boundary. As a rule, the development of the intranuclear cascade was not calculated accurately enough (in particular, none of the studies performed so far took into account changes in the properties of the target nucleus with growing cascade particle shower); in many studies the meson production process was neglected, and calculation of the competition between the processes of evaporation and fission of the excited nuclei resulting from the cascade stage of the interaction was based on some rather arbitrary assumptions on the evaporation to fission width ratio Γ_n / Γ_f, or very crude theoretical estimates for the Γ_n / Γ_f value were employed. This resulted in a low accuracy of the calculations, and, besides, it remained unclear what was responsible for disagreement with experiment: either the substantial defects of the model proper or the roughness of the approximations employed [9].

The Monte-Carlo methods developed at our Laboratory for calculating intranuclear cascades allow one to get good agreement with experiment over the wide energy range from several

tens of MeV up to several hundred GeV [9-13] *). On the other hand, with the help of the semiphenomenological approximation for fission barriers, considered in refs.[13,15] it is possible to obtain the Γ_n / Γ_f values for a wide range of mass and charge numbers A and Z, which are in good agreement with experiment. A combination of these results allows one to hope for a considerable expansion of the area of the applicability of the interactions of fast particles with heavy fissioning nuclei and for an increase in the accuracy of calculations. This particular problem is the main subject of the present paper.

In the model of high-energy nuclear fission, two independent aspects can be singled out, namely, 1) the formation of a fissioning nucleus as a result of the intranuclear cascade and of the subsequent competition with the particle evaporation process, and 2) the fission mechanism proper which is responsible for the properties of decay products. In order to be able to make sufficiently definite predictions and indicate the points where the theory should be improved in the first place, it is important to know to what extent the model under consideration agrees with experiment in each of these aspects.

*) The joint group at the Brookhaven National Laboratory and the Columbia University has developed a rather detailed cascade model for an energy region below the threshold of meson production, while at the Oak Ridge National Laboratory the same has been done for energies up to several GeV. Our results agree with the data of these groups rather well[14].

Now we shall restrict ourselves to only the first aspect without touching at all upon the fission mechanism, which is a problem even in the region of low energies.

In our calculations we make use of the model of a nucleus with the diffuse Woods-Saxon boundary and take into account the law of energy-momentum conservation in each of the intranuclear pion- and nucleon-nucleon collisions. At all energies T of primary particles we take into account the effect of depletion of the nuclear density in the course of the cascade (the "trailing" effect). The details of the cascade calculations are the same as in refs. [9-11].

For calculation of the width ratio Γ_n / Γ_f we take advantage of the method described in papers [13,15]. In order to avoid obscuring the essence of the matter by introducing a large number of parameters, we assume the values of the level density parameters to be the same in both evaporating and fissioning nuclei, namely $a_n = a_f = a \cdot A$ MeV^{-1}, and the value of a to include no corrections due to the shell structure of the decaying nucleus and to be independent of its excitation energy. In the case of high energy reactions to be considered, such an approach is a good enough approximation, since intranuclear cascades are followed by the formation of a large set of residual nuclei with different characteristics, and then the effective averaging of the parameter a over the excitation energies E^* of these nuclei, their mass and charge numbers, A and Z, takes place. Nevertheless, we shall see later that in order to get agreement with experiment one should assume the a value to decrease somehow with increasing A.

All the errors in theoretical results, to be indicated below, are purely statistical and do not include the errors due to inaccuracies in the models themselves.

2. THE FISSION CROSS SECTION

The fission cross section σ_f is defined by the ratio of the number N_f of fission events to the total number N_t of Monte-Carlo simulations. However in the case of low-fissioning nuclei (e.g., gold) $N_f \ll N_t$ and, as a consequence, a large number of cascades should be calculated to obtain the value of σ_f with sufficient statistical accuracy. As a result, the calculation of the fission cross section becomes extremely time-consuming. We have carried out Monte-Carlo sampling by means of the statistical weight functions $W_n = \prod_{i=1}^{N} \omega_{ni}$ and $W_f = 1 - W_n$, where W_n is the Monte-Carlo calculated probability for the nucleus to "drop" the excitation energy E^* by the chain (cascade) of N successive evaporations of particles; W_f is the probability for the nucleus to fission at one of the chain stages; $\omega_{ni} = 1 - \omega_{fi}$ is the probability of particle emission at the i-th stage of the evaporation cascade; ω_{fi} is the corresponding fission probability which is easy to determine using the expressions for the ratios Γ_n / Γ_f from ref.[15]. After the subsequent averaging of the W_f value over the total number N_{in} of the cascades followed, and the multiplication of the result by the corresponding total cross section σ_{in} for inelastic interactions, we obtain the fission cross section for the nucleus at a given projectile energy T: $\sigma_f = \sigma_{in} \sum_{i=1}^{N_{in}} (W_f)_i / N_{in}$. (The cross section σ_{in} is also calculated by the Monte-Carlo method, i.e., $\sigma_{in} = \sigma_{geom} \cdot N_{in} / N_t$).

The variation of the cross sections σ_f with the target-nucleus mass number and primary proton energy T is shown in figs. 1 and 2.

It is seen that the theoretical curves reproduce well all the main features of the experimental dependences. In particular, the slowing down increase in the cross sections at high energies in the case of low-fissioning nuclei and the decrease in cross sections with increasing energy T for heavy fissioning nuclei are explained by the fact that, as energy T becomes higher, the residual nuclei left after the cascade stage are lighter while the fission barriers are higher. As a consequence, the probability for their fission becomes smaller.

It should be noted that the correct energy dependence $\sigma_f(T)$ can be obtained in case one assumes the fission barrier B_f to decrease with increasing excitation energy E^*. Because of the absence of any sufficiently convincing considerations about the energy dependence of $B_f(E^*)$, as an estimate we used the relation $B_f(E^*) = B_f/(1+\sqrt{E^*/2A})$, which makes it possible to get

agreement with experiment in the region of $T < 1$ GeV[*] within the accuracy of the known experimental data. It is seen from table I to what extent it is important to take into account the energy dependence $B_f(E^*)$.

At $T \gg 1$ GeV for all nuclei the fission cross section becomes a slowly varying function of energy. The anomalies of the curves $\sigma_f(A)$ in fig. 1 are associated with variations in the ratio Γ_n / Γ_f as a result of shell corrections in the vicinity of the double magic nucleus with A = 208.

---

[*] The fission barrier can be divided into two parts, namely a smooth "liquid-drop" part and that due to shell effects and corrections for pairing. General considerations suggest that the contribution from the latter part decreases with increasing E^*, while the problem of the energy dependence of the smooth part is less clear. In ref.[45] by means of the classical thermodynamics the relation $B_f(E^*) = B_f (1-E^*/E_0^*)$ was obtained, where $E_0^* = at_0^2$, $t_0 \simeq 9$ Mev. In the region of moderate energies the results obtained with this relation are slightly different from ours (see also ref.[46]); however at high energies, $E^* \gtrsim E_0^*$, the estimates of ref.[45] cannot be used.

As regards the Coulomb barrier, its energy dependence was chosen to be of the form $V_c(E^*) = V_c / (1+\sqrt{E^* / 2A})$ as well.

The calculated cross sections appear to be rather close to experimental ones provided the value of $a_f = a_n \simeq A/10 + A/15$ MeV^{-1} is chosen for the level density parameter, the best agreement is obtained for nuclei with $Z > 90$ if a is chosen to approach the last value.

Attention is attracted by the large scatter of the measured results σ_f, especially at $T \gtrsim 1$ GeV. The data[16,17] obtained using mica detectors seem to be most accurate (in fig. 2 they are marked with ■ and ●).

The calculated fissilities of the nuclei σ_f / σ_{in} (see fig. 3) are also in good agreement with experiment[**].

In accordance with the anomaly in the dependence $\sigma_f(A)$ in the vicinity of A=208 the fissilities of the two neighbouring nuclei ^{207}Pb and ^{209}Bi shown in fig. 3 differ nearly by a factor of one and a half.

3. THE YIELD OF INDIVIDUAL ISOTOPES

The extent of agreement between the calculated and experimental values is seen from figs. 4–8, where the data on the isotopic yield for uranium and bismuth targets are given as typical examples.

Since the calculation of the yield of individual isotopes requires a large amount of computer time, the accuracy of the theoretical data given in figs. 4–8 is not very high.

[**] For determination of the experimental values of σ_f / σ_{in} the statistically analysed experimental cross sections σ_{in} from the review [26] have been used.

In particular, the irregular behaviour of the calculated curves in going from one value of A to the neighbouring ones is practically completely due to statistical fluctuations. The calculation errors are close to the average value of these fluctuations. Like the calculation for the fission cross sections σ_f, the Monte-Carlo calculation of the yield of individual isotopes, which requires the selection of rather rare events, has been carried out using the weights W_f and W_n.

Within the calculation errors the theoretical and experimental data shown in figs. 4–8 are rather close; the behaviour of the experimental cross sections is reproduced correctly in the interval of a few orders of magnitude.

In comparison with the calculations neglecting the boundary diffusity, the accuracy of predictions for reactions with a smaller number of fast cascade particles, e.g., for the reactions $^{238}U(p, pxn)^{238-x}U$, is substantially increased. This result is entirely clear, since such reactions are, in the main, associated with the cascade process on the periphery of the nucleus.

If the fission of the excited residual nuclei is neglected and their decay is assumed to be due to the evaporation process, the calculated results agree with experiment only for a group of nearest isotopes (the number of neutrons emitted $x \lesssim 3$–5) and appear to be enhanced largely (sometimes by several orders of magnitude) for the remaining isotopes.

The calculated curves shown in figs. 4–8 are related

to the level density parameter $a_n = a_f = A/15$ MeV^{-1} *). A decrease in this parameter (within the limits $\simeq$ (A/15–A/20) reduces the relative contribution from the fission process (see fig. 3) and the calculation turns out to be closer to the experimental points. However we did not so far carry out a detailed fitting of the a-parameter value. (A more extensive study of this parameter as a function of A, Z and E^* is our next task).

Figs. 4–7 show for comparison also the data calculated by Hahn and Bertini [8] under the assumption that in the region of $Z \gtrsim 88$, the Sikkeland approximation [31] is applicable to the width ratio Γ_n / Γ_f, while none of the residual nuclei with $Z \lesssim 88$ undergo fission. As has been indicated in refs.[15,32] the Sikkeland approximation is related to the Γ_n / Γ_f value averaged over the evaporation cascade, i.e., over a wide range of excitation energy E^*. This is the reason why the Γ_n / Γ_f ratio depending sharply on excitation energy turns out to be E^* -independent in the Sikkeland approximation. This is clearly a very crude approximation, but in calculating the characteristics averaged over E^* one may hope for a rather good applicability of the Sikkeland approximation since the intranuclear cascades initiated by high-energy particles give rise to residual nuclei with a wide range of the E^* values. This is just an explanation of the fact that the curves of

*) This value of the level density parameter will also be used in the two following sections.

Hahn and Bertini, shown in figs. 4 and 5, are in sufficiently good agreement with the experimental points (in some cases even better than our results; see, e.g., fig.5). In considering some more detailed characteristics that are functions of E^*, the use of the Sikkeland approximation may yield results by several orders of magnitude different from the experimental ones.

4. ACCOMPANYING PARTICLES

The properties of the particles emitted by nuclei, which subsequently undergo fission, are described well in the framework of the cascade-evaporation model.

Fig. 9 shows the multiplicity distributions $N_n = N(n)/\sum_n N(n)$ of the charged component of these particles (mainly of protons since at $T < 1$ GeV the contribution from π-mesons and other particles is still small[9]). Figs. 9 and 10 show the corresponding values of the particle average multiplicity $\langle n \rangle = \sum_n n\, N(n) / \sum_n N(n)$. The theoretical and the experimental data do not differ within the limits of statistical errors. For comparison the results of Hahn and Bertini[8] are also presented in fig.10. At $T \lesssim 1$–2 GeV their data are rather close to the results of our calculations, but they have a pronounced tendency for a considerably more rapid increase, and at $T \gtrsim 2$ GeV their results already substantially exceed our data. This difference is conditioned by the fact that in ref.[8] no account is taken of the effect of a decrease in the density of the number of intranuclear nucleons as the cascade shower develops, and this effect leads to the flattening of the dependence of excitation energy E^* and all related characteristics on the energy T of primary particles (see section 5 below).

The values of the average neutron multiplicity are listed in fig. 10. Since we do not here give consideration to the fission process itself (see section 1 above), the calculated multiplicity includes only the neutrons produced in the course of the cascade stage and those neutrons which were evaporated from the excited residual nucleus prior to its fission. The experimental multiplicity includes, in addition, the neutrons emitted from excited fission fragments and, therefore, considerably exceeds the calculated value [*] (especially at low energies, $T \sim 100$ MeV).

Similarly to the case of protons, the calculated multiplicity of neutrons from ref.[8] increases too rapidly in the region of $T \gtrsim 1$–2 GeV.

In figs. 11 and 12 comparison is made with experiment of the angular and energy distributions of particles accompanying the fission process. Here the experimental data are in good agreement with theory as well.

5. THE PROPERTIES OF RESIDUAL NUCLEI

Figs. 13–15 show the distributions of residual nuclei over their excitation energy E^*, and mass and charge numbers, A and Z. The distributions $W_c(E^*_{fc})$ and $W_f(E^*_f)$ correspond, respectively, to the excited fissioning nuclei at the moment immediately following the cascade stage of the interaction and at the moment just prior to their fission, i.e., when these

[*] If fission neutrons are taken into account, $\langle n \rangle_{theor} \cong \langle n \rangle_{exp.}$, as it has been shown in the model neglecting target-nucleus diffusity[2,9]. The value of $\langle n \rangle$ is slightly affected by taking into account the diffusity of the nuclear boundary.

nuclei have already lost a considerable amount of their excitation energy. For comparison the distributions $W_p(E^*_p)$ for residual nuclei that did not undergo fission and de-excited only by particle emission are also given. The excitation energy distribution for all events after the completion of the cascade stage is defined by the sum $W(E^*) = (\sigma_f / \sigma_{in}) W_c(E^*) + (1-\sigma_f / \sigma_{in}) W_p(E^*)$.

The figures show that before fissioning the nucleus, as a rule, decreases its energy by particle evaporation*).

The average energy $\langle E^* \rangle$ increases rapidly with increasing energy of the primary particle. At $T \gtrsim 1$-3 GeV, owing to the "trailing effect", the quantity $\langle E^* \rangle$ becomes practically constant. For instance, for the interaction p + ^{238}U at T=10 and 20 GeV the average energy $\langle E^* \rangle$ of nuclei after the intranuclear cascade is equal to 365 ± 25 MeV and 376 ± 25 MeV, respectively.

Although for nuclei heavier than gold the quantity $\langle E^* \rangle$ is practically independent of the target nucleus, the values of $\langle E^*_{fc} \rangle$ for these nuclei change rather noticeably, e.g., at T=660 MeV for bismuth $\langle E^*_{fc} \rangle = 203 \pm 18$ MeV, while for uranium $\langle E^*_{fc} \rangle = 111 \pm 3$ MeV, i.e., the excitation energy $\langle E^*_{fc} \rangle$ of the fissioning nucleus decreases as one moves towards the heavier targets.

*) It is noteworthy that a similar behaviour is characteristic of not only nuclei with A ≲ 238, but also of very heavy excited nuclei produced in the collisions of ions with nuclei [43].

Table 2 shows that the experimental values of $\langle E^*_{fc} \rangle$ are close to the theoretical ones while the latter are relatively slightly dependent on the level density parameter. (The distributions shown in figs. 13-15 are calculated for $a_n = a_f = A/15$ MeV^{-1}).

As to distributions of residual nuclei over their charge and mass numbers, they have a considerably larger dispersion for heavy target nuclei, which increases with increasing energy T until the moment when in the region of energies exceeding several GeV this growth is slowed down by the "trailing" effect. In view of the fact that an excited nucleus, prior to fission, emits usually one or several particles, the distributions of pre-fission nuclei appear to be considerably wider than those immediately after the cascade stage of the process. In other words, before fissioning the nucleus becomes usually "colder" and lighter.

Fig. 16 shows the calculated distribution of the residual nuclei over their mass numbers to agree well with experiment both in shape and in the absolute value of the yield cross section $\sigma(A)$. Unless the competition with the fission process is included, one does not succeed in obtaining agreement with experiment.

6. CONCLUSION

A comparison of the experiment and theory shows that the mechanism of intranuclear cascades including the competing processes of fission and particle evaporation of excited residual nuclei gives good fit to the available experimental data on interactions of high-energy particles with fissioning

nuclei. As a rule, the accuracy of calculations of averaged quantities and average distributions turns out to be not lower than that of experimental measurements. The calculated values are rather slightly dependent on uncertainties in the choice of model parameters. In the region of energies of $T \gtrsim 1$ GeV it is very important to take into account the "trailing" effect.

Noticeable differences between the experiment and theory are observed only in the cross sections for the yield of individual isotopes, where the theory needs further improvement and experiment should be more accurate.

The model considered can, in principle, be used successfully in applied calculations associated with the penetration of high-energy radiation through fissionable media [44].

The authors are thankful to S.A.Karamyan for helpful discussions and critical comments.

References

1) R.G.Vasilkov, V.I.Goldansky, V.P.Dzhelepov. V.P.Dmitrievsky, Atomnaya Energiya 29 (1970)151
2) V.S.Barashenkov, V.M.Maltsev, V.D.Toneev, Izv. AN SSSR, fizika, 30(1966)322,337
3) M.Lindner and A.Turkevich, Phys.Rev. 119(1960)1632
4) B.D.Pate and A.M.Poskanzer, Phys.Rev. 123(1961)647
5) Y.LeBeyec, M.Lefort, J.Peter, Nucl.Phys. 88(1966)215
6) J.J.Hogan and N.Sugarman, Phys.Rev. 182(1969)1210
7) E.Cheifetz, Z.Fraenkel, J.Galin, M.Lefort, J.Peter, X.Tarrago, Phys.Rev. 2C(1970)256
8) R.L.Hahn and H.W.Bertini, Phys.Rev. 6C(1972)660
9) V.S.Barashenkov and V.D.Toneev, The interaction of high-energy particles and nuclei with nuclei"(Atomizdat, Moscow, 1972)
10) V.S.Barashenkov, A.S.Iljinov, N.M.Sobolevsky, V.D.Toneev, JINR Comm. P2-5507(1970), E2-5813(1971)
11) V.S.Barashenkov, A.S.Iljinov, V.D.Toneev, Yad.Fiz. 13(1971)743
12) V.S.Barashenkov, S.M.Eliseev, JINR Comm. P2-6395(1972), Yad.Fiz.(in press)
13) V.S.Barashenkov, K.K.Gudima, F.G.Gereghi, A.S.Iljinov, V.D.Toneev, JINR Comm. E2-6706(1972)
14) V.S.Barashenkov, H.W.Bertini, K.Chen, G.Friedlander, G.D.Harp, A.S.Iljinov, J.M.Miller, V.D.Toneev, Nucl.Phys. A187(1972)531
15) V.S.Barashenkov, F.G.Gereghi, A.S.Iljinov, V.D.Toneev, JINR Comm. P7-6741(1972); Nucl.Phys. A206(1973)131
16) R.Brandt, F.Carbonara, E.Cieslak, H.Piekarz, J.Piekarz and J.Zakrzewski, The study of nuclear fission induced by high-energy protons, CERN Preprint, 1970
17) J.Hudis and S.Katcoff, Phys.Rev. 180(1969)1122
18) V.A.Konshin, E.S.Matusevich, V.I.Regushevsky, Yad.Fiz. 2(1965)682
E.S.Matusevich, V.I.Regushevsky, Yad.Fiz.7(1968)1187
19) H.G.de Carvalho, G.Potenza, R.Rinzivilli, E.Sassi and G.Vanderhaeghe, Nuovo Cimento 25(1962)880

H.G.de Carvalho, G.Cortini, M.Muchik, G.Potenza, R.Rinzivilli and W.O.Lock, Nuovo Cimento 27(1963)468
20) N.S.Ivanova, JETP 31(1956)413
21) V.S.Bychenkov, N.A.Perfilov, Yad.Fiz. 5(1967)264
22) N.A.Perfilov, JETP 41(1961)871
23) E.Hyde, I.Perlman, G.Seaborg, Nuclear fission (Atomizdat, Moscow, 1969)
24) N.A.Perfilov, V.F.Darovskikh, G.F.Denisenko, A.I.Obukhov, JETP 38(1960)716
25) A.K.Lavrukhina, L.D.Krasavina, At.Ener. 2(1957)27
26) V.S.Barashenkov, K.K.Gudima, V.D.Toneev, JINR Communications P2-4183(1968)
27) M.Lindner and R.N.Osborne, Phys.Rev. 103(1956)378
28) A.K.Lavrukhina, S.S.Rodin, Radiokhimiya 2(1960)83
29) B.Pate and A.Poskanzer, Phys.Rev. 123(1961)647
30) B.I.Belyaev, A.V.Kalyamin, A.N.Murin, Izv. AN SSSR, ser.fizika 27(1963)923
31) T.Sikkeland, A.Ghiorso, M.J.Nurmia, Phys.Rev.172(1968)1232
32) V.S.Barashenkov, F.G.Gereghi, A.S.Iljinov, V.D.Toneev, JINR Comm. P7-6619(1972)
33) N.S.Ivanova, I.I.Pyanov, JETP 31(1956)416
34) E.Cheifetz, Z.Fraenkel, J.Galin, M.Lefort, J.Peter and X.Tarrago, Phys.Rev. 2C(1970)256
35) M.Bercovitch, H.Garmichael, G.C.Hanna and E.P.Hincks, Phys.Rev. 119(1960)412
36) W.E.Crandall and G.P.Millburn, J. Appl.Phys.29(1958)698
37) R.G.Vasilkov, B.B.Govorkov, V.I.Goldansky, V.A.Konshin, O.S.Lupandin, E.S.Matusevich, B.A.Pimenov, S.S.Prokhorov, S.G.Tsypin, Yad.Fiz.7(1968)88
38) N.A.Perfilov, Fission physics of atomic nuclei (Atomizdat, Moscow, 1957) p.98
39) N.S.Ivanova, Fission physics of atomic nuclei (Atomizdat, Moscow, 1957) p.215

40) V.P.Shamov, Fission physics of atomic nuclei (Atomizdat, Moscow, 1957) p.129
41) V.P.Shamov, DAN SSSR 103(1955)593
42) N.Sugerman, W.Muenzel, J.A.Panontin, K.Wielgoz, M.V.Romanian, G.Lang, E.Lopez-Mencharo, Phys.Rev. 143(1966)952
43) V.S.Barashenkov, F.G.Gereghi, A.S.Iljinov, V.D.Toneev, JINR Comm. P7-6798(1972)
44) V.S.Barashenkov, V.D.Toneev, JINR Comm. P16-6623(1972)
45) Y.Yamaguchi, Prog.Theor.Phys. 6(1951)529
46) I.Dostrovsky, Z.Fraenkel, P.Rabinovitz, Proc. of the 2nd UN Intern. Conf. on the Peaceful Uses of Atomic Energy, Geneva, 1958 v.15, p.301

Received by Publishing Department
on July 2, 1973

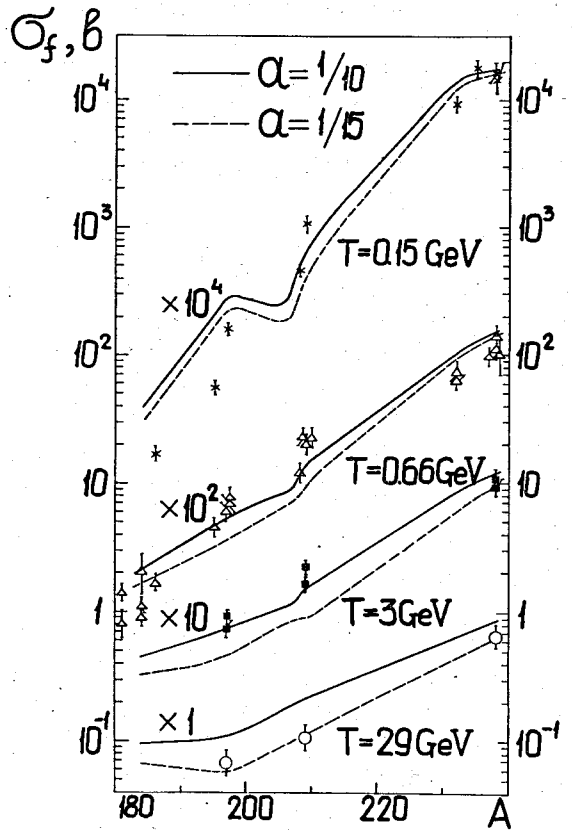

Fig.1. The fission cross section for a nucleus with mass number A, bombarded by protons with energy T. The solid and dashed curves correspond to calculations at different values of the level density parameter $a_n = a_f = a$ A MeV^{-1}. The statistical errors of the calculated data are about 7%. The experimental points are from refs.[16-22].

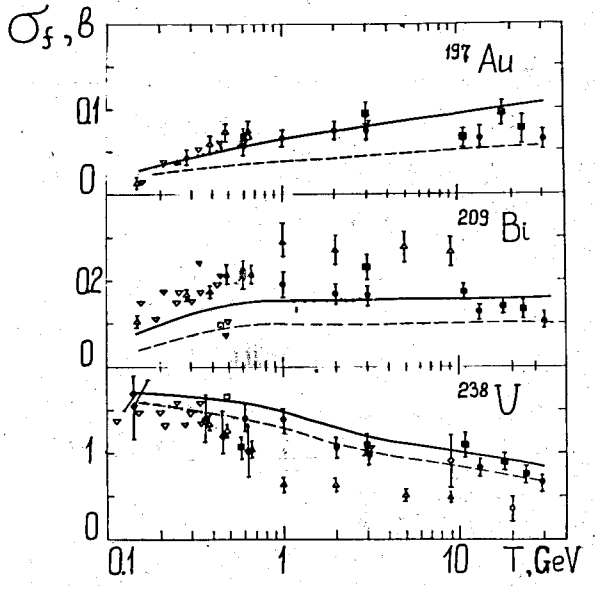

Fig.2. The energy dependence of fission cross sections for the nuclei of gold, bismuth and uranium, bombarded by protons with energy T. The solid and dashed curves are calculations for a =1/10 and a =1/15, respectively. The statistical errors of the calculated results are about 7%. The marks ■, ●, △, ○, ◆, ▽, ◇, and □ designate the experimental points from refs.[16-20,23-25], respectively.

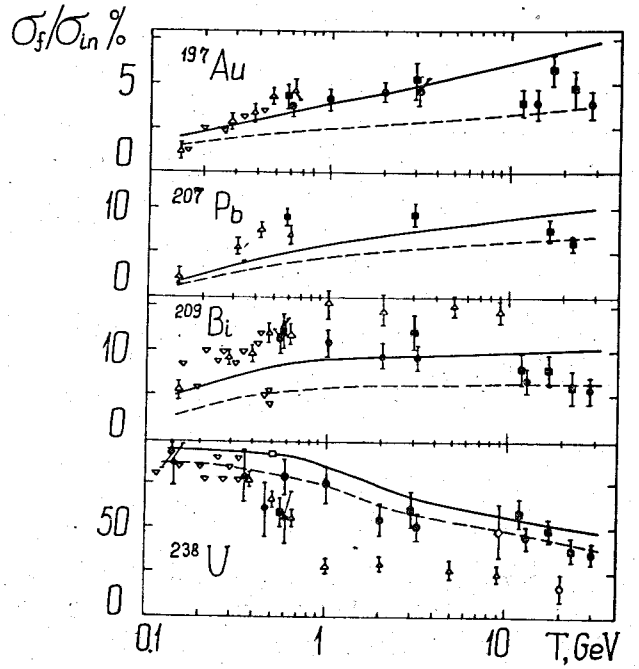

Fig.3. Nuclear fissility as a function of the energy T of primary protons. Designations are the same as in fig.2.

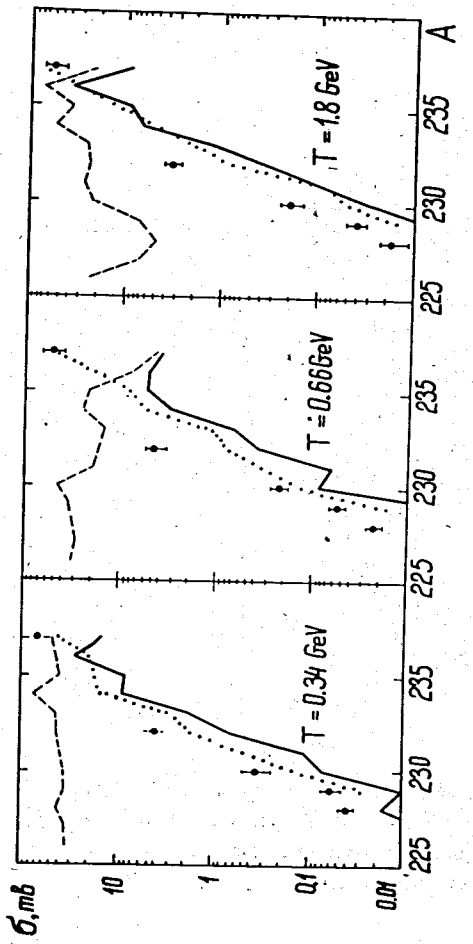

Fig.4. The yield of uranium isotopes in the reaction $^{238}U(p,pxn)^{238-x}U$ at different energies T of primary protons. The solid and dashed curves correspond to calculations with and without fission taken into account. The dotted lines are theoretical data from ref.[8]. The experimental points are taken from refs.[27-29].

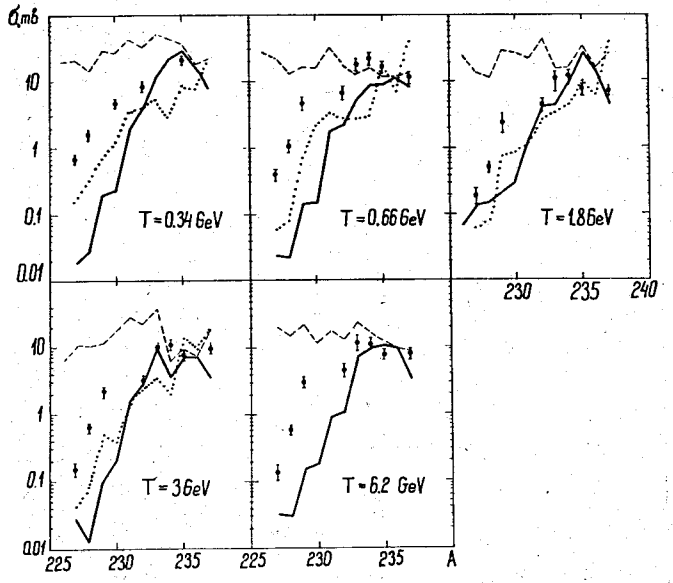

Fig.5. The yield of protactinium isotopes in the reaction $^{238}U(p,2pxn)^{238-x}Pa$ at different energies T of primary protons. Designations are the same as in fig.4. The experimental points are from refs.[27-29].

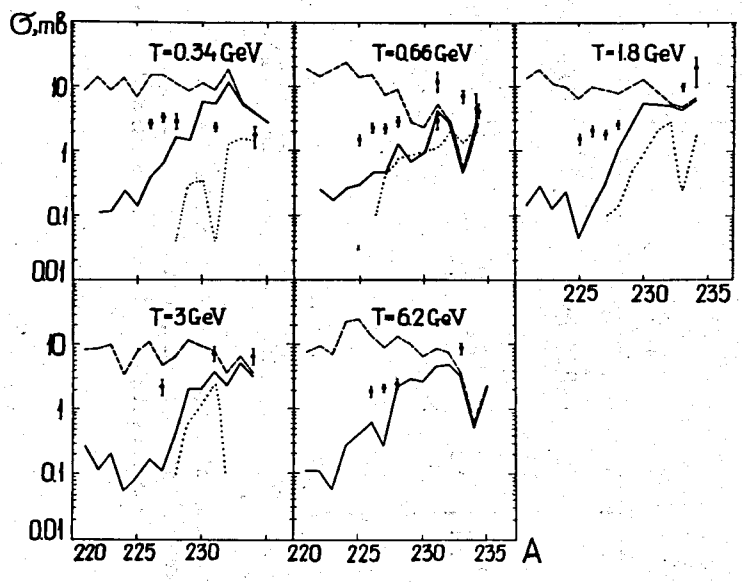

Fig.6. The yield of thorium isotopes in the reaction $^{238}U(p,3pxn)^{236-x}Th$. All designations are the same as in fig.4. The experimental points are from refs.[27-29].

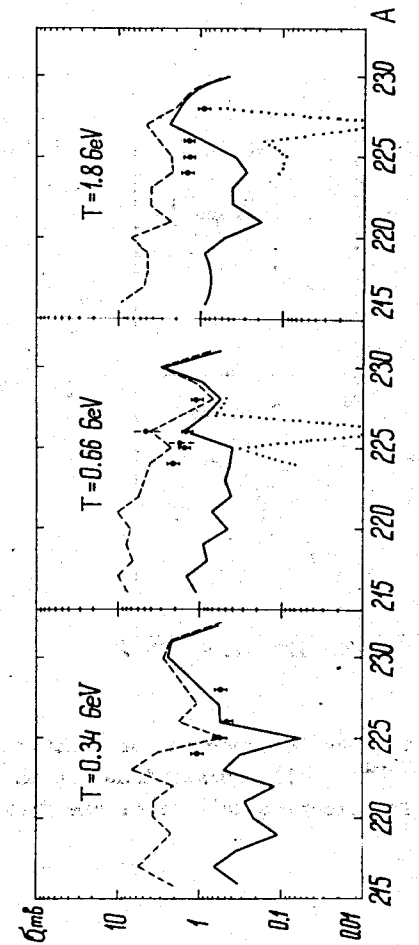

Fig.7. The yield of actinium isotopes in the reaction $^{238}U(p,4pxn)^{235-x}Ac$. All designations are the same as in fig.4. The experimental points are from refs.[27-29].

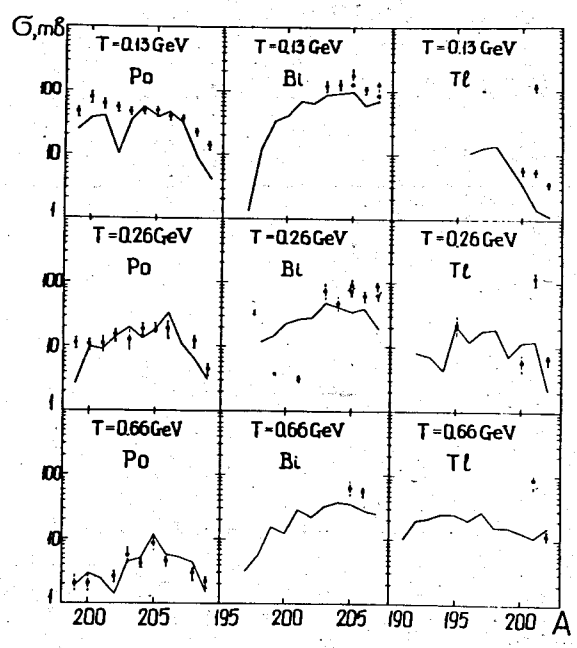

Fig.8. The yield of polonium, bismuth and thallium isotopes in the reactions $^{209}Bi(p,xn)^{210-x}Po$, $^{209}Bi(p,pxn)^{209-x}Bi$ and $^{209}Bi(p,3pxn)^{204-x}Tl$ at energy T of primary protons. The curves are calculated results, the experimental points are from ref.[30].

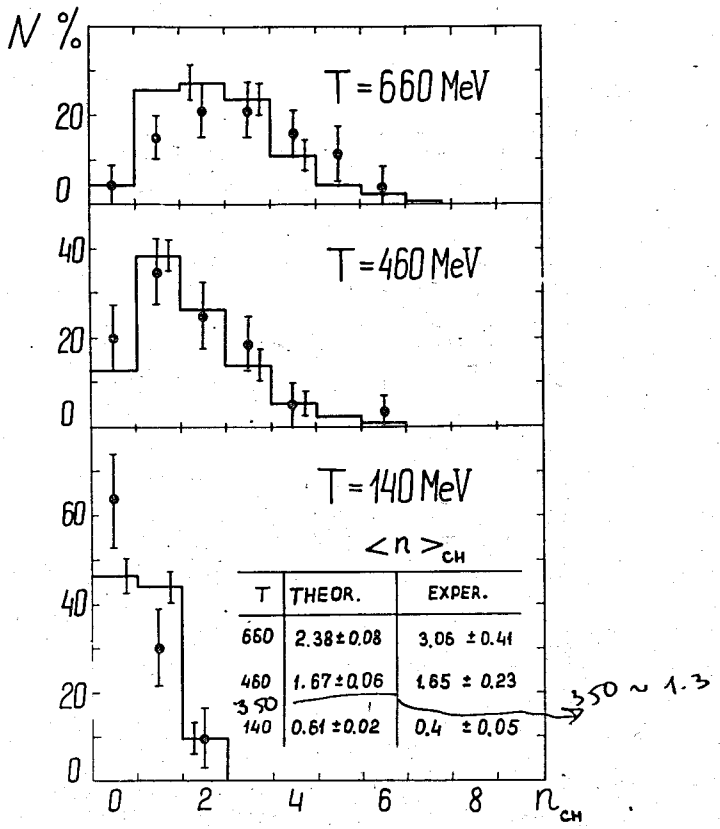

Fig.9. The distribution of the fissioning nuclei from ^{238}U over the number of charged particles produced. T is the energy of primary protons. The histograms are calculated results, the experimental points are from ref.[33]. The corresponding experimental and theoretical values of the average multiplicity $\langle n \rangle_{CH}$ are also given.

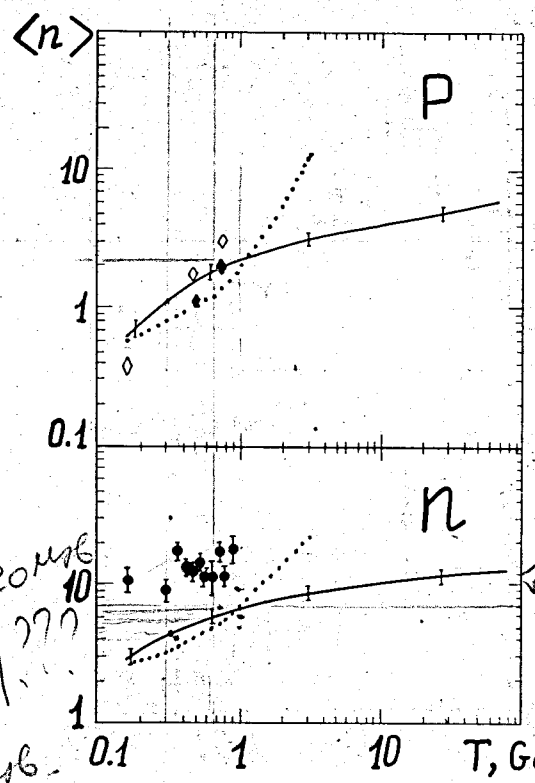

Fig.10. The average multiplicities of protons and neutrons (the upper and the lower parts, respectively) resulting from events with the fission of the ^{238}U target-nuclei, induced by protons with energy T. The solid and dotted curves are our calculated results and the data from ref.[8], respectively. The experimental points are taken from refs.[33-38]; the open marks ◇ in the upper part are the total multiplicity of all protons generated, while the shaded marks ◆ correspond only to cascade protons[33,38].

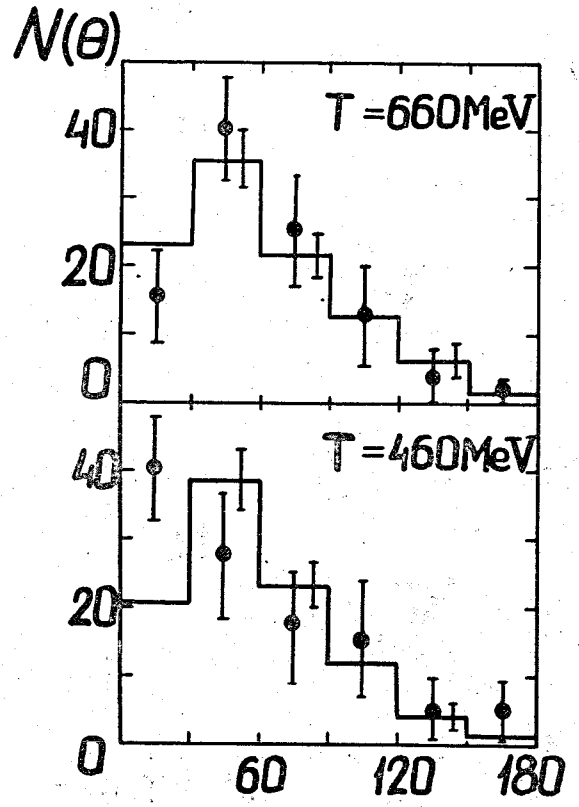

Fig.11. The angular distribution of charged particles with an energy higher than 20 MeV, accompanying the fission of the ^{238}U nuclei, induced by protons with energy T. The histograms represent calculated results, the points are experimental ones from ref.[39].

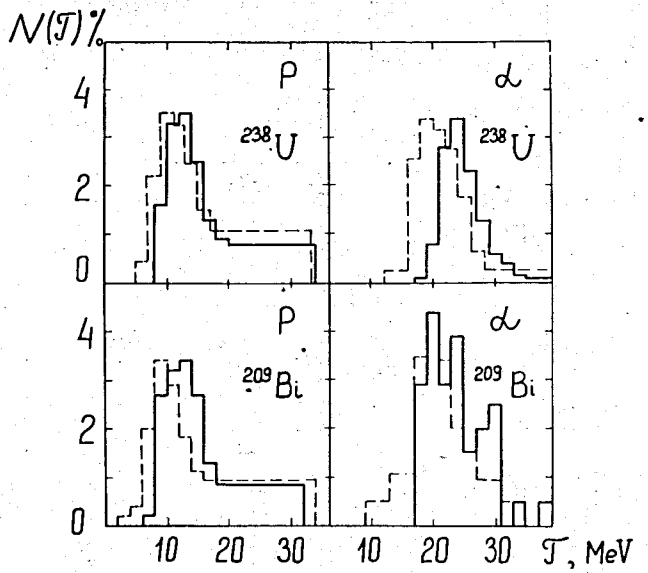

Fig.12. The energy distribution of protons and alpha-particles accompanying the fission of uranium and bismuth nuclei, induced by 660-MeV protons. The solid histograms are our calculated results, the dashed ones are experimental data from ref.[40].

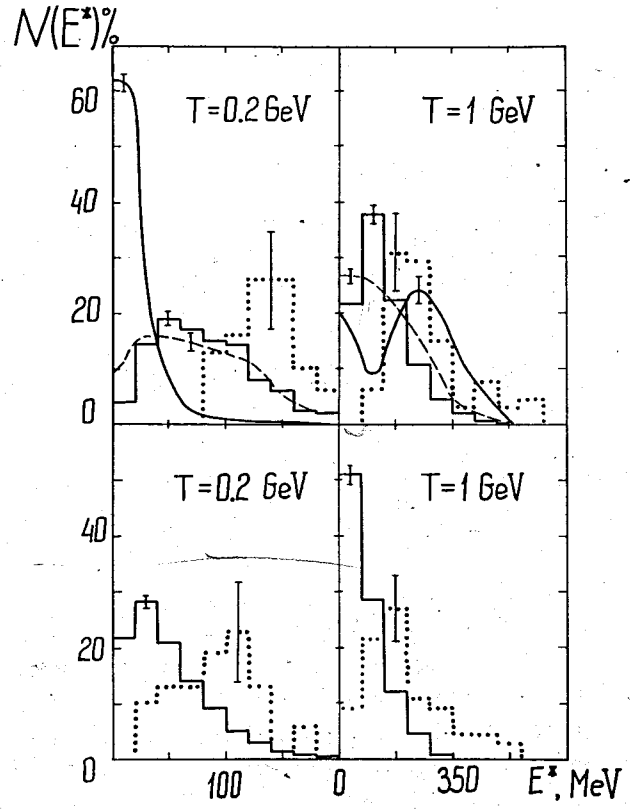

Fig.13. The excitation-energy distribution for residual nuclei immediately after the intranuclear cascade (two upper plots) and prior to fission (two lower plots). The histograms are results for fission events, the curves (in the upper plots) correspond to events without fission. The solid histograms and curves are the data for the reaction p+^{238}U, whereas the dashed curve is the data for the reaction p+^{197}Au. The energy of primary protons is equal to 0.2 and 1 GeV.

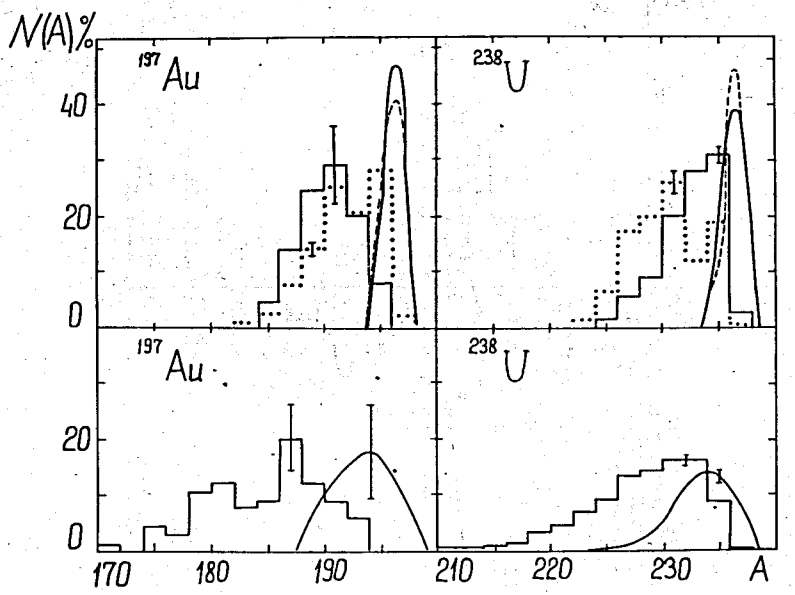

Fig.14. The distribution over the mass numbers of the residual nuclei generated in the reactions p+^{197}Au and p+^{238}U, immediately after the intranuclear cascade (two upper plots) and prior to fission (two lower plots). The solid curves and histograms are calculated results for the nuclei that underwent fission, the dashed curves and dotted histograms (in the upper plot) correspond to events without fission. The histograms show the data for T=1 GeV, the curves represent the corresponding data for T=0.2 GeV.

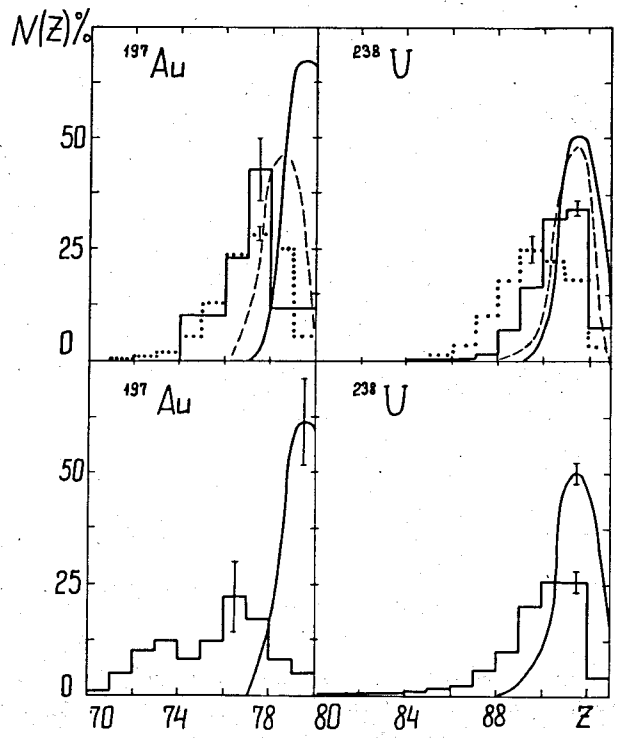

Fig.15. The charge distribution of the residual nuclei produced in the reactions p+^{197}Au and p+^{238}U at energies T=0.2 and 1 GeV. The upper plots correspond to the nuclei at the moment immediately after the cascade stage of the process, while the lower plots concern pre-fission nuclei. Designations are those used in fig.14.

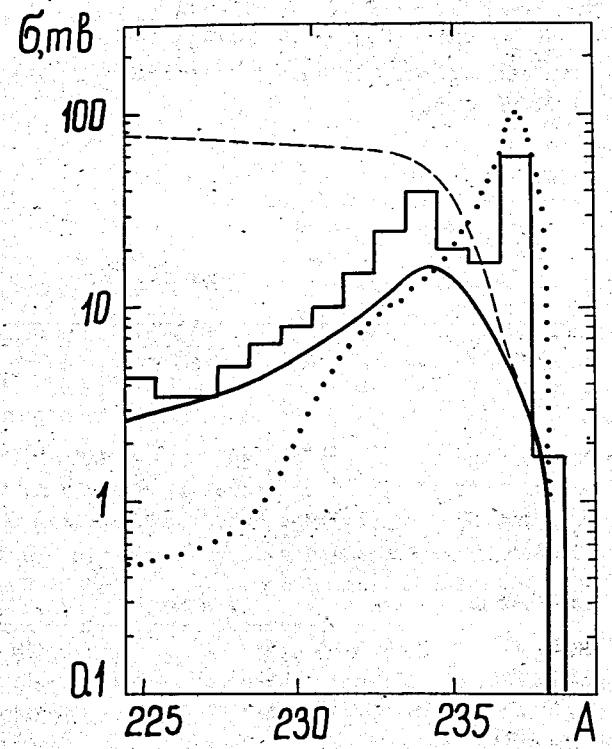

Fig.16. The yield of residual nuclei in bombardment of the ^{238}U nuclei with protons with energy T=1.8 GeV, as a function of their mass numbers. The solid and dashed curves correspond to calculations with and without the fission process, respectively. The dotted curve represents the calculated results of ref.[8]. The statistical errors of calculations are about 10%. The histogram represents the experimental data from ref.[29].

TABLE I. The cross sections σ_f(mb) for the fission of uranium and gold isotopes, induced by protons with energy T with and without the energy dependence of fission barriers $B_f(E^*)$.

Nucleus	T,GeV 0.2	1	10	Barrier
$^{197}Au_{79}$	30.5 ± 1.8	65.4 ± 3.9	105.6 ± 6.3	$B_f(E^*)$
	0.69 ± 0.04	3.04 ± 0.18	4.40 ± 0.26	$B_f(E^*=0)$
$^{238}U_{92}$	1578 ± 95	1379 ± 83	835 ± 50	$B_f(E^*)$
	1215 ± 73	800 ± 48	482 ± 29	$B_f(E^*=0)$

TABLE II. The average excitation energy $\langle E^*_{fc}\rangle$ MeV of the nuclei left after the intranuclear cascade in the reaction p+^{238}U. Only the nuclei that underwent fission have been selected.

T, MeV	Experiment	Theory $a = 1/10$	Theory $a = 1/15$
140	80 ± 20 [33]	76 ± 7	76 ± 7
350	140 ± 40 [33]	103 ± 10	90 ± 9
460	130 [42]	110 ± 11	108 ± 10
	135 ± 15 [42]		
	165 ± 45 [33]		
660	175 ± 17 [21]	138 ± 14	136 ± 13
	150 [42]		
	185 ± 60 [33]		